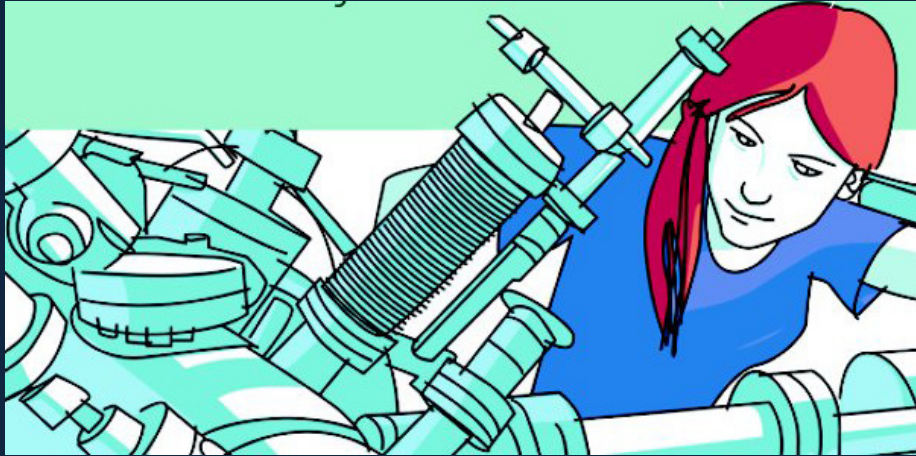


Morphology, structure and interface properties in metal/oxide systems

Paola Luches

S³, Istituto Nanoscienze
Consiglio Nazionale delle Ricerche
Modena
Italy



overview

1. cerium oxide ultrathin films on Pt(111)



growth of Ag nanoparticles

- introduction
- morphology, composition and structure
- the CeO₂/Pt interface

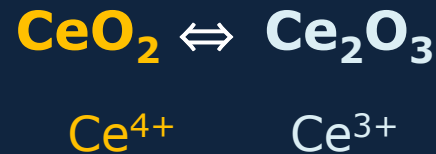
2. the Fe/NiO interface

- introduction
- depth-resolved magnetic characterization by NRS

cerium oxide

store, transport and release oxygen

oxydizing conditions



reducing conditions

The image shows a standard periodic table of elements. The element Cerium (Ce) is highlighted with a red circle. It is located in the lanthanide series, which is part of the f-block. The table also shows other elements like Lanthanum (La), Praseodymium (Pr), Neodymium (Nd), and others in the same series. The atomic number of Ce is 58, and its symbol is Ce. The table also includes the atomic mass and phase (Solid, Liquid, Gas) for many elements.

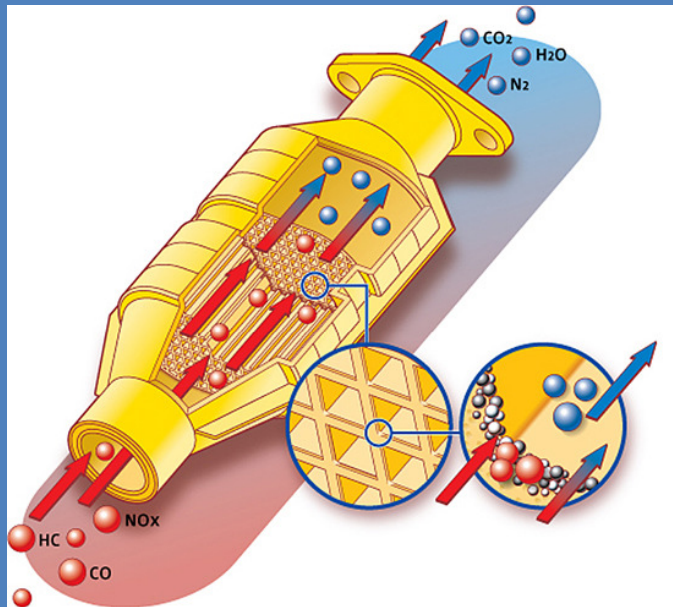


+ metals

- supported nanoparticles (Pt, Ag, Au, Rh,...)
- dopants (Sm, Gd, La,...)

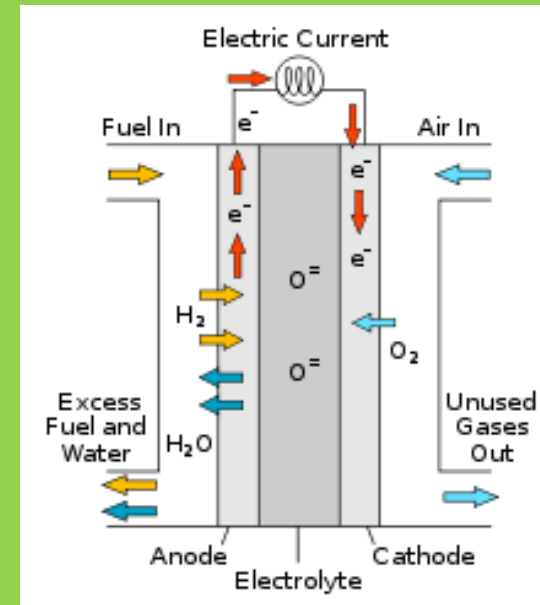
cerium oxide

catalytic converters



- oxidize CO to CO₂
- reduce NO_x to N₂
- self clean from C deposits

solid-oxide fuel cells



- solid electrolyte
high conductivity for O ions
- production of hydrogen
water gas shift
thermochem. water splitting

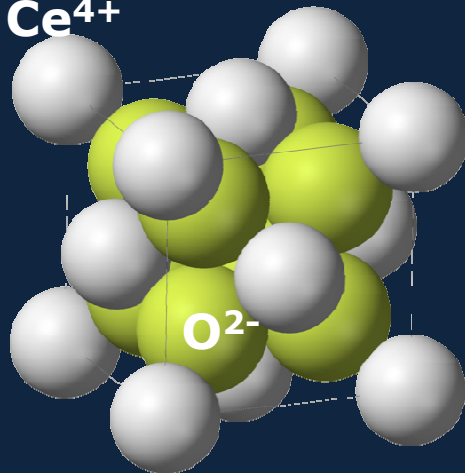
cerium oxide

model systems \Rightarrow understand and optimize the properties

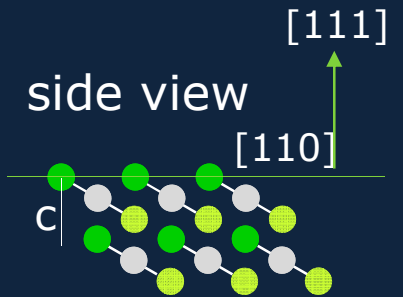
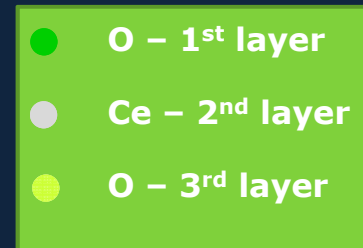
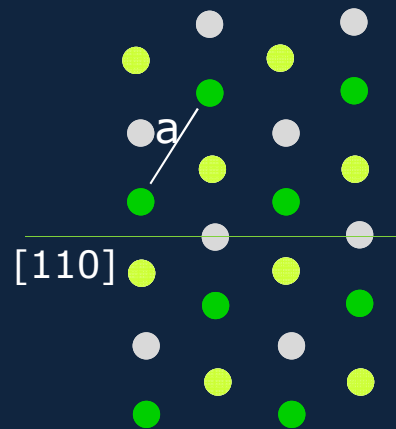
CeO₂

CaF₂ - structure

Ce⁴⁺



(111) surface
top view



$$c_{\text{CeO}_2} = 3.124 \text{ \AA}$$

$$a_{\text{CeO}_2} = 3.826 \text{ \AA}$$

previous studies

Surface Science 600 (2006) 5004–5010
 Morphology and defect structure of the CeO₂(111) films grown on Cu(111) as studied by scanning tunneling microscopy
 J. Phys. Chem. C 2008, 112, 20012–20017 · Shaikhutdinov ^{a,*}, H.-J. Freund ^a

Surface Science 520 (2002) 173–185
 CO Oxidation on a CeO₂/Pt(111) Inverse Model Catalyst Surface: Catalytic Promotion and Tuning of Kinetic Phase Diagrams
 Y. Suchorski ^{a,*}, R. Wrobel ^{a,†}, S. D. ...

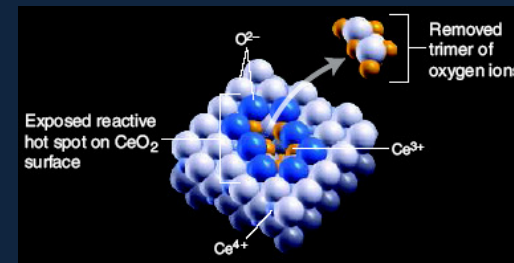
Surface Science 603 (2009) 3382–3388
 EPR route to continuous ultra-thin cerium oxide films on Cu(111)
 Thorsten Staudt ^a, Yaroslava Lykhach ^a, Lutz Hammer ^b, M. Alexander Schneider ^b, Vladimir Matolin ^c, Jörg Libuda ^{a,*}

Surface Science 309 (2005) 752
 Electron Localization Determines Defect Formation on Ceria Substrates
 Friedrich Esch, et al.
 S. Eck, C. Castellani

PRL 99, 056101 (2007)
 Surface Oxygen Vacancy Ordering on Reduced CeO₂(111)
 ... and Michael Reichling

open points

1. oxygen vacancy formation mechanism

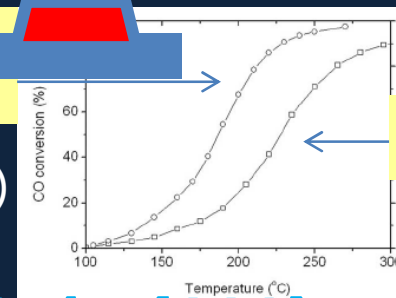


F. Esch et al., Science 309 (2005) 752

2. metal/oxide interaction



3. stabilization of surfaces different from (111)

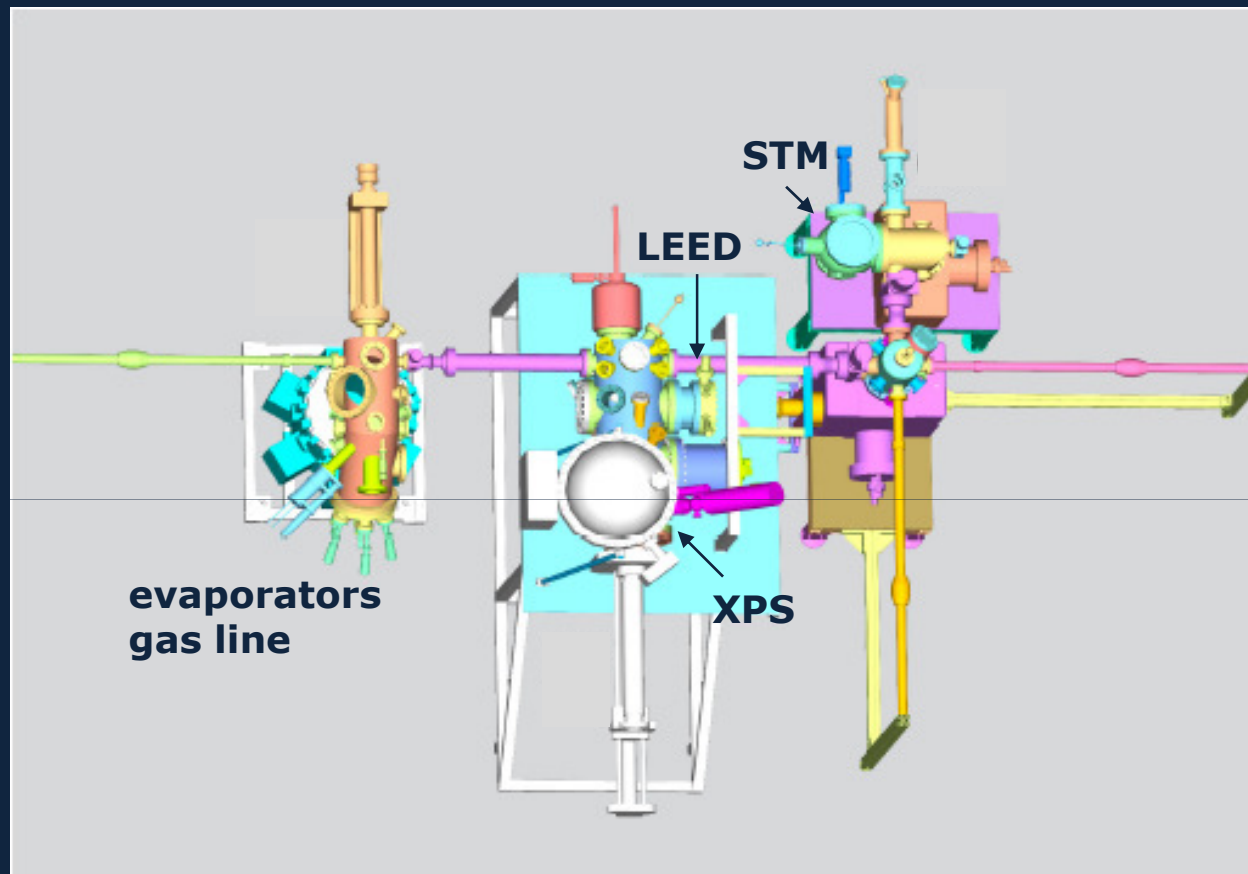


np exposing mainly {111}

⇒ XPS, STM, LEED study of CeO₂/Pt(111)

Zhou et al., J. Cat. 299 (2005) 206

experimental



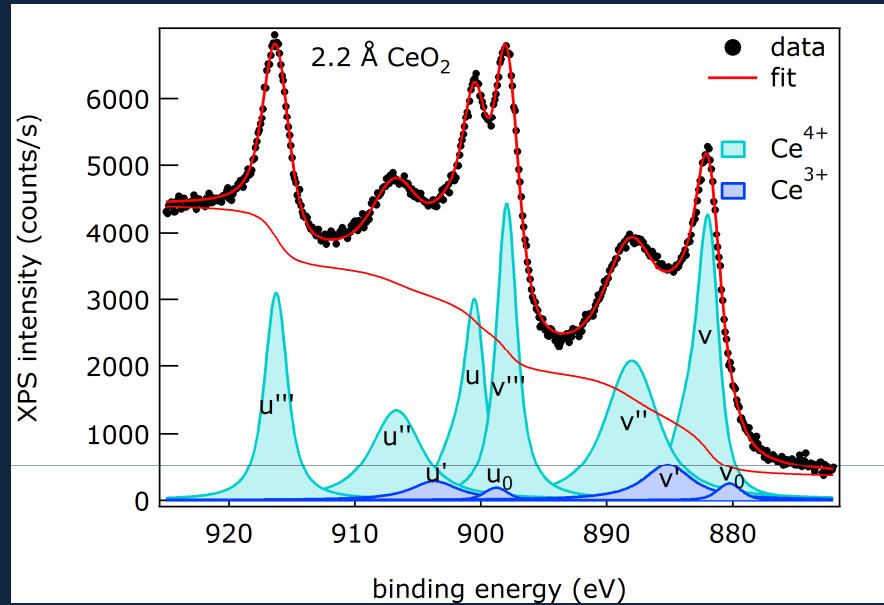
substrate

Pt(111) → $a_{\text{Pt}} = 2.775 \text{ \AA}$
 $a_{\text{CeO}_2} = 3.826 \text{ \AA}$ m=38%

CeO₂ growth conditions

$R_{\text{Ce}} = 3 \times 10^{-3} \text{ \AA/sec}$ @ RT
 $P_{\text{O}_2} = 1 \times 10^{-7} \text{ Torr}$

Ce 3d XPS

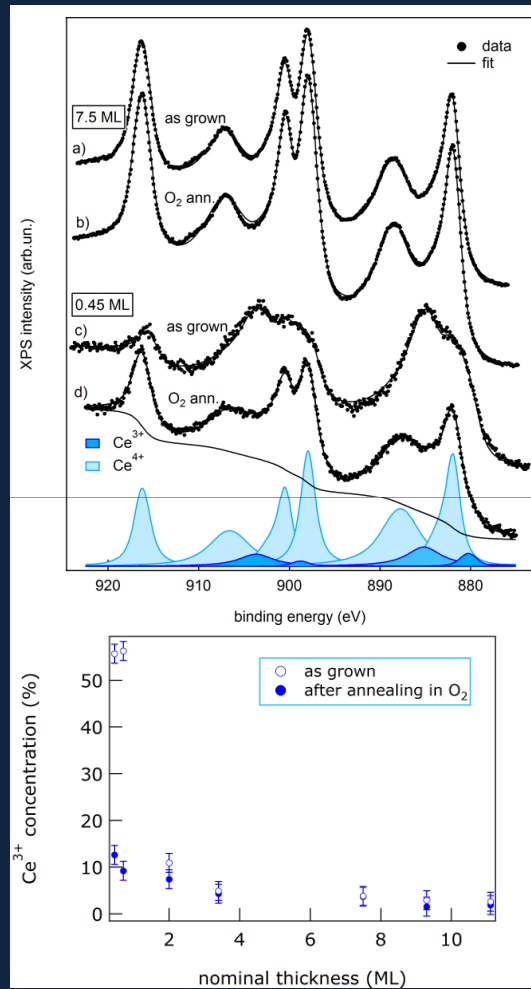


ION	Initial state	Final state	peak
Ce ³⁺	3d ¹⁰ 4f ¹	3d ⁹ 4f ² V ⁿ⁻¹	v ⁰ , u ⁰
	3d ¹⁰ 4f ¹	3d ⁹ 4f ¹ V ⁿ	v', u'
Ce ⁴⁺	3d ¹⁰ 4f ⁰	3d ⁹ 4f ² V ⁿ⁻²	v, u
	3d ¹⁰ 4f ⁰	3d ⁹ 4f ¹ V ⁿ⁻¹	v'', u''
	3d ¹⁰ 4f ⁰	3d ⁹ 4f ⁰ V ⁿ	v''', u'''

M. Romeo, et al. Surf. Interface Anal. 20 (1993) 508.
Skala et al. J. Electron Spectrosc. Rel. Phen. 169 (2009) 20

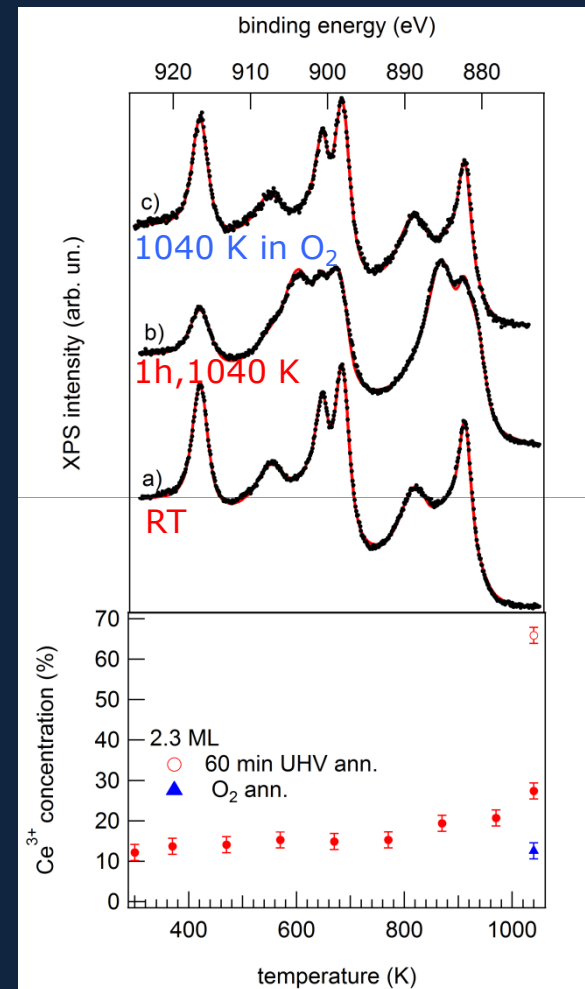
stoichiometry

Ce 3d XPS



**annealing @1040 K in O₂
oxidizes the films**

Ce 3d XPS



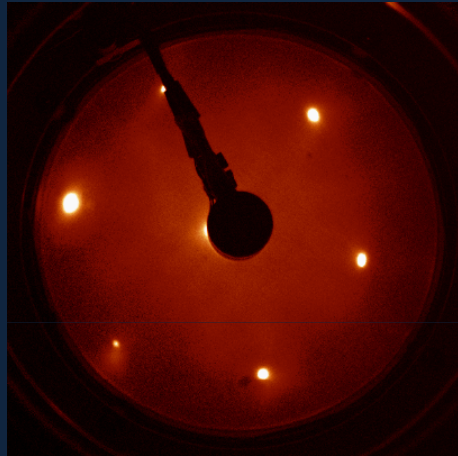
**annealing in UHV reduces
the films**

structure

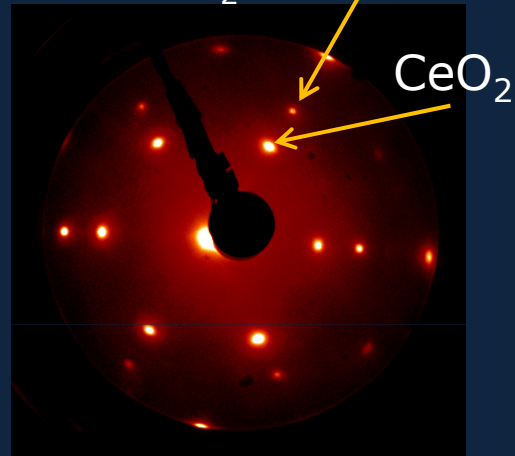
LEED

$E=80$ eV

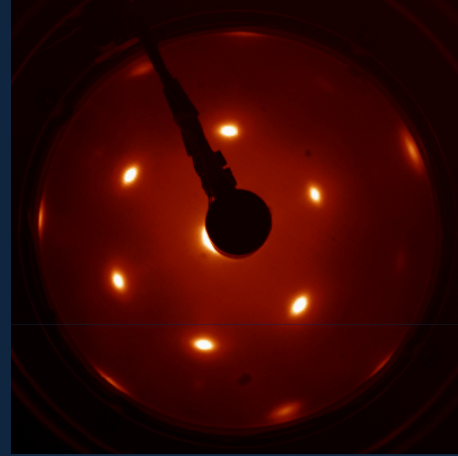
clean Pt(111)



2 ML CeO_2



11 ML CeO_2



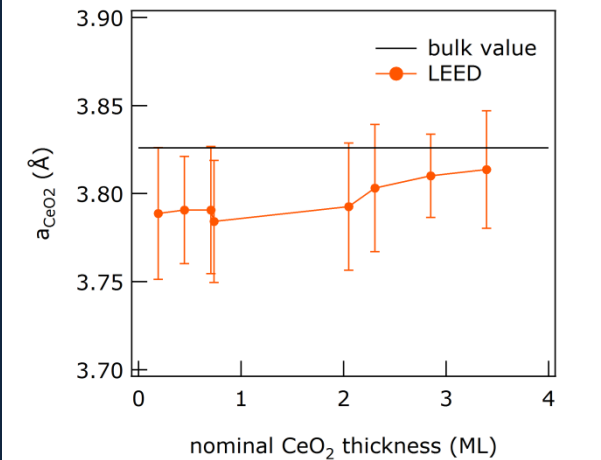
$$a_{\text{CeO}_2} = 3.826 \text{ \AA}$$

$$a_{\text{Pt}} = 2.775 \text{ \AA}$$

$$m = 38\%$$

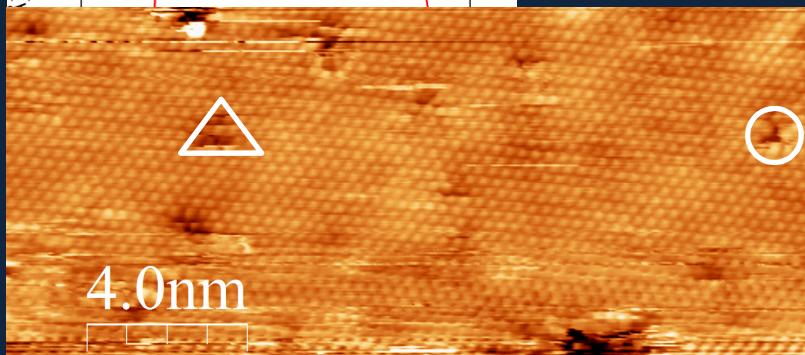
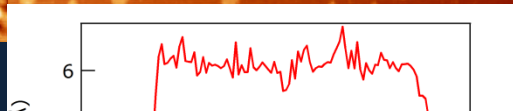
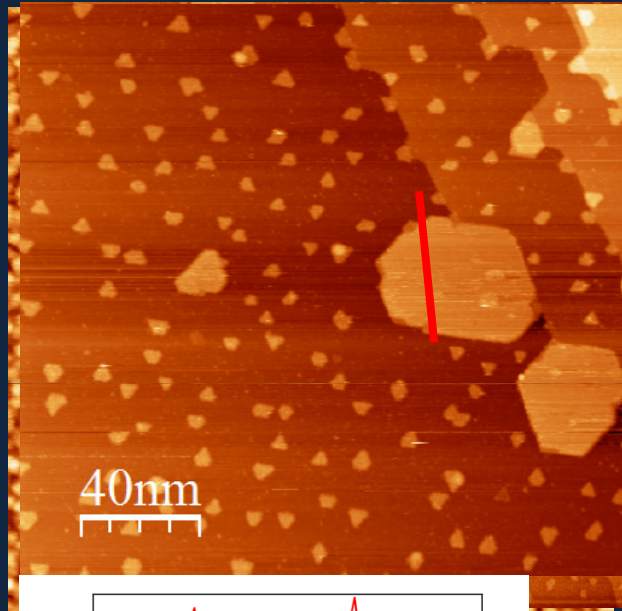
epitaxial films

$(111) \text{ CeO}_2$
 $\langle 110 \rangle_{\text{CeO}_2} // \langle 110 \rangle_{\text{Pt}}$



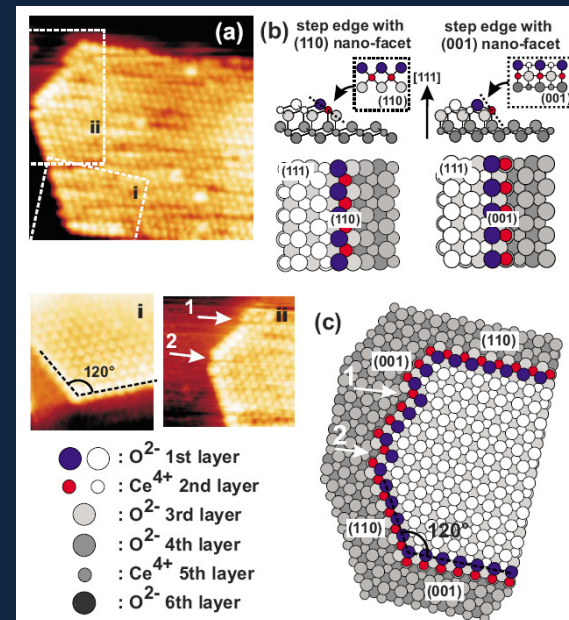
morphology

20ML Pt deposited on Pt(111) CeO_2



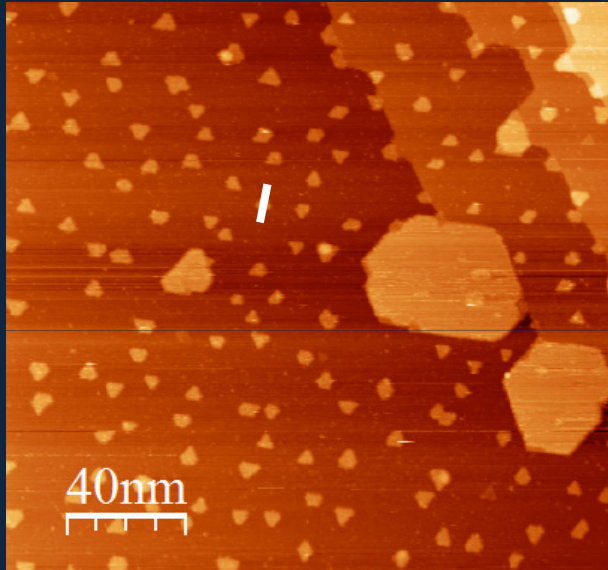
1. Large islands $\rightarrow \text{CeO}_2$

- 30-50 nm wide
- 6 Å (2 O-Ce-O ML) high
- atomically flat
- preferentially at Pt step edges
- straight edges, kinks at 120°



morphology

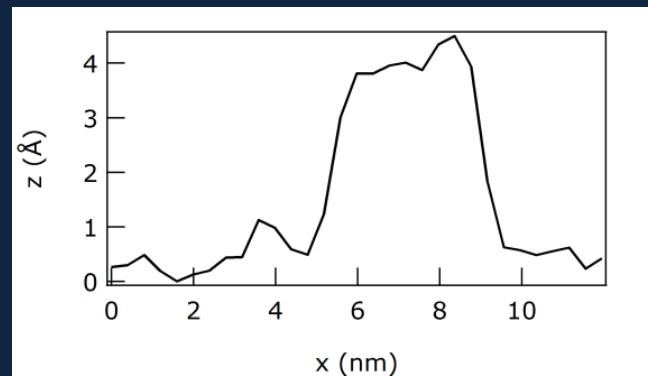
0.2 ML ann. 1040 K O₂



0.5 V 0.2 nA

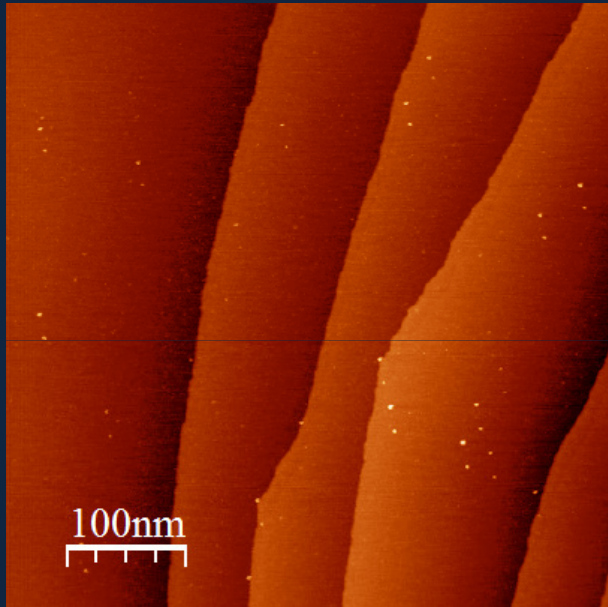
1. Small islands

- ~ 5 nm wide
- ~ 3 Å high
- atomically flat
- uniformly distributed
- triangular shape (kinks at 60°)

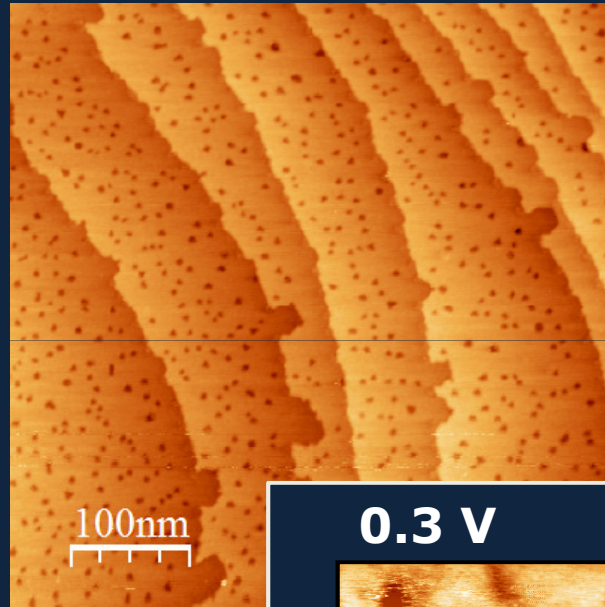


morphology

clean Pt(111)

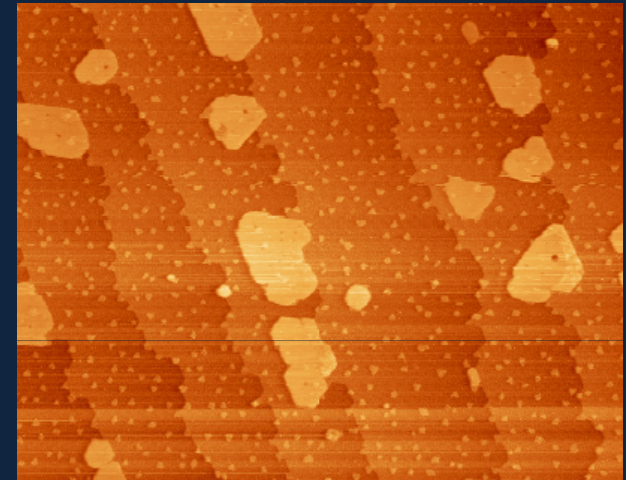


Pt (111)
ann. @ 1040 K O₂

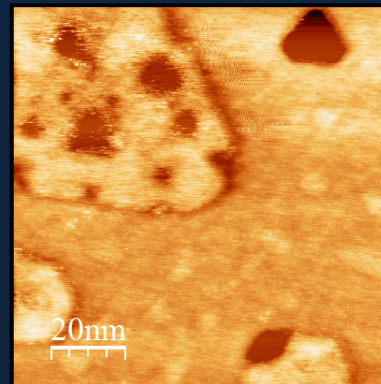


0.5 V 0.1 nA

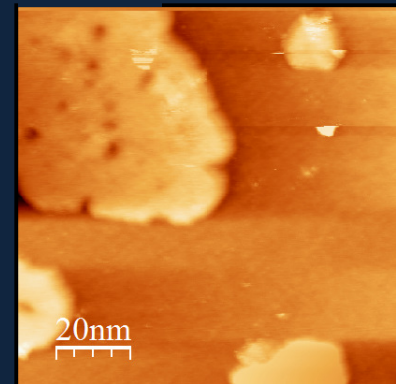
0.2 ML CeO₂
ann. @ 1040 K O₂



0.3 V



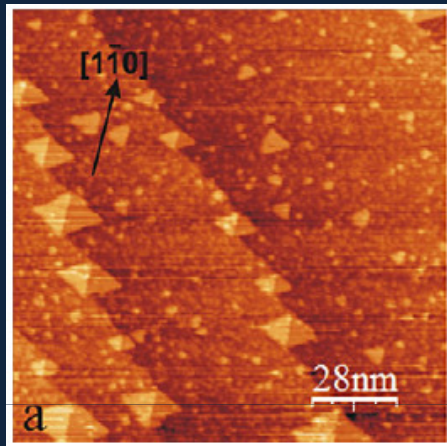
1 V



0.7 ML CeO₂ 0.1 nA

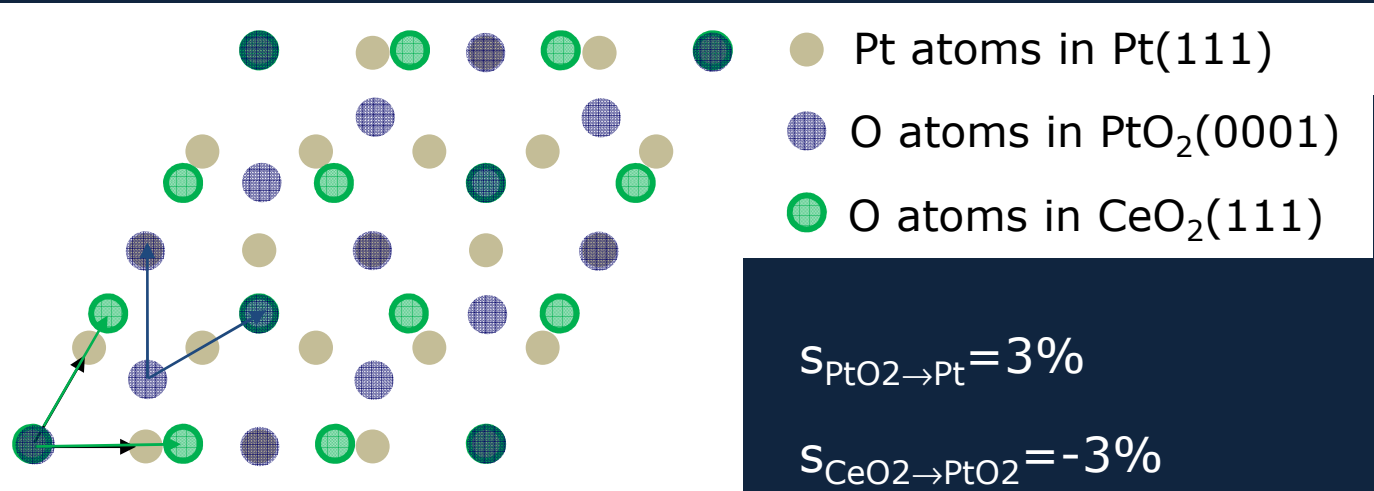
morphology

α -PtO₂(0001) nanoislands

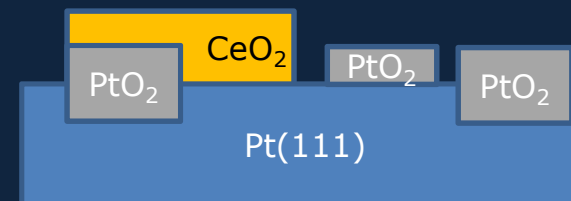


S.A. Karsnikov et al.
Nanotech. 21 (10) 335301

$$a_{\text{Pt}} = 2.78 \text{ \AA}$$
$$a_{\text{PtO}_2} = 3.12 \text{ \AA}$$
$$a_{\text{CeO}_2} = 3.83 \text{ \AA}$$

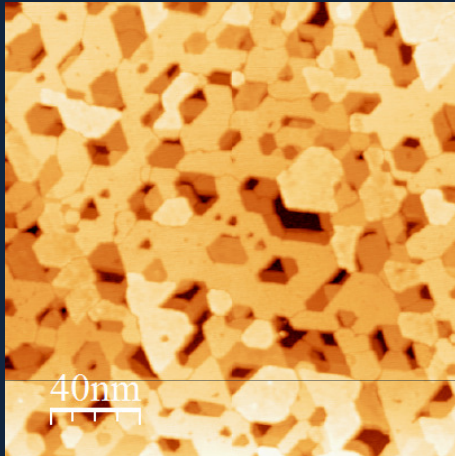


PtO₂ islands may act as a template for the stabilization of CeO₂ in the observed epitaxial orientation

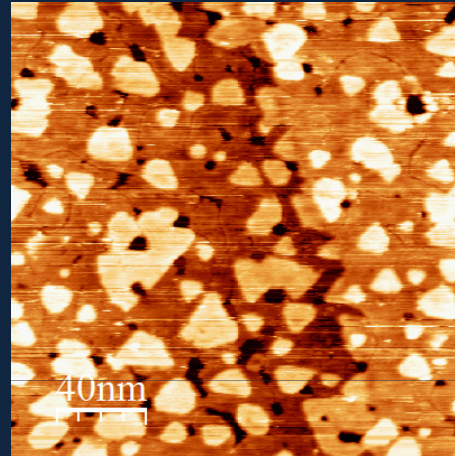


morphology

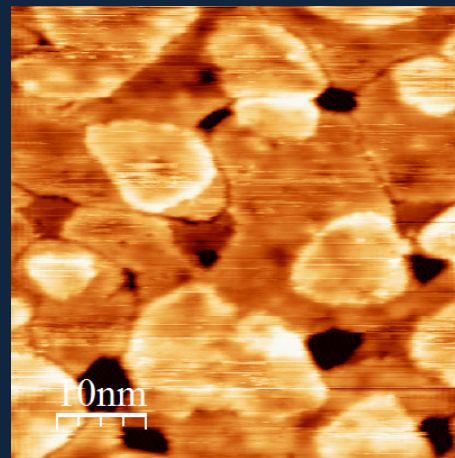
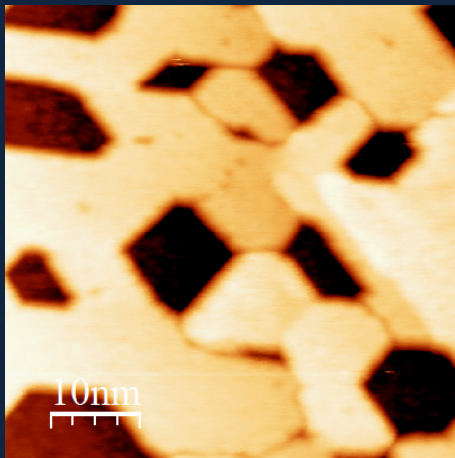
3.4 ML CeO₂



9.3 ML CeO₂

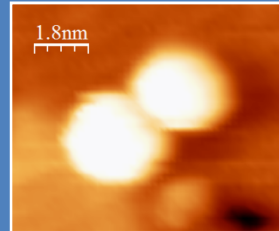
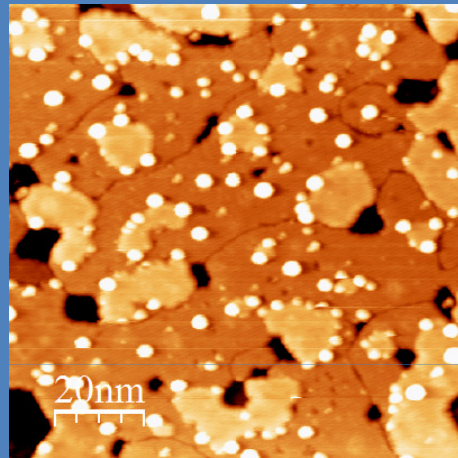
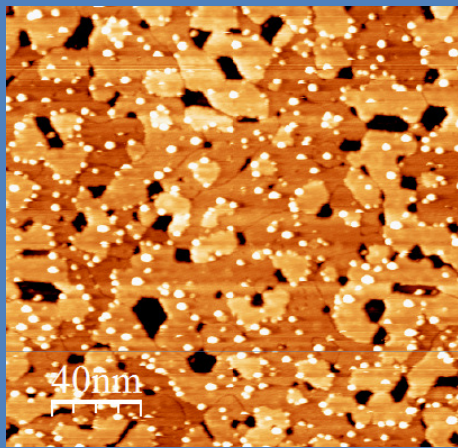


- flat CeO₂ terraces
- straight edges 120°
- linear defects



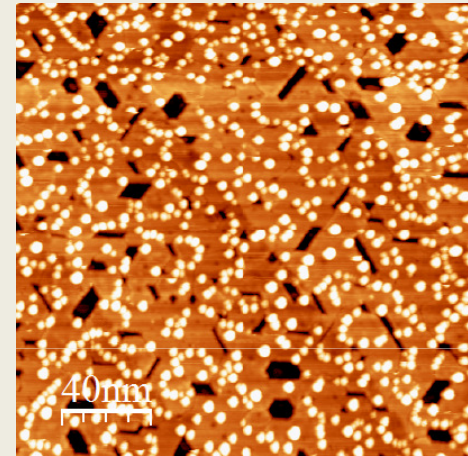
Ag/CeO₂

0.07 Å Ag / 3 ML CeO₂



d=0.5-3nm
h=0.5-1 nm

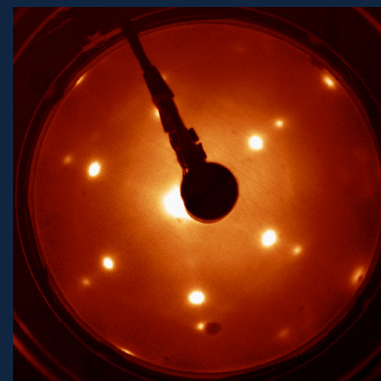
0.2 Å Ag / 3 ML CeO₂



d= 2-5 nm
h=0.5-2 nm

- decoration of CeO₂-CeO₂ steps
- hexagonal shape → (111) orientation

epitaxy



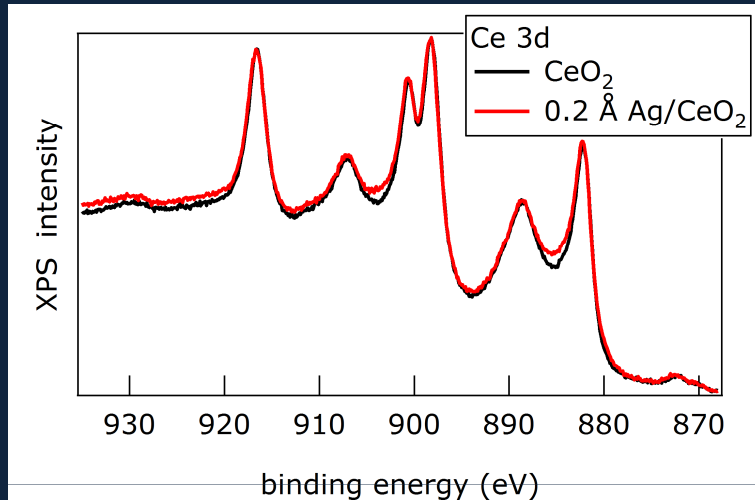
Ag film on CeO₂

$a_{\text{CeO}_2} = 3.826 \text{ \AA}$

$a_{\text{Ag}} = 2.892 \text{ \AA}$

m=32%

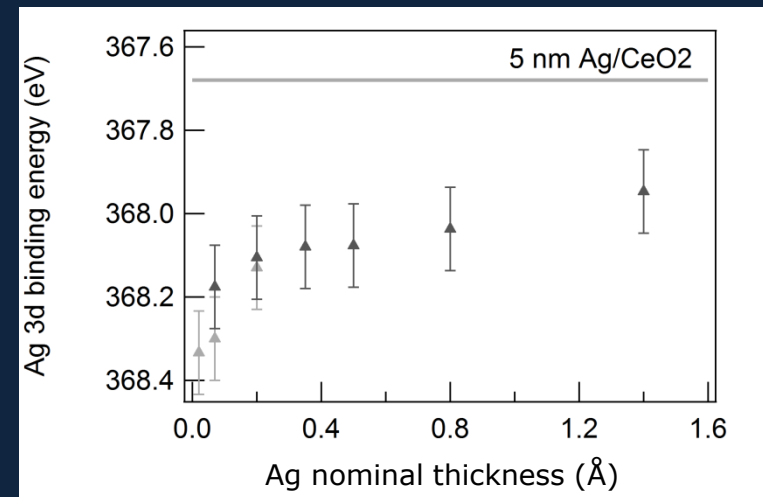
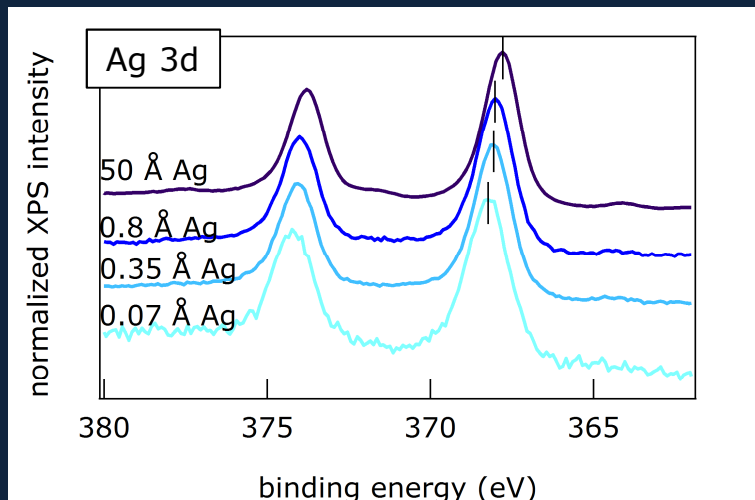
Ag/CeO₂



ceria reduction

higher Ag 3d BE

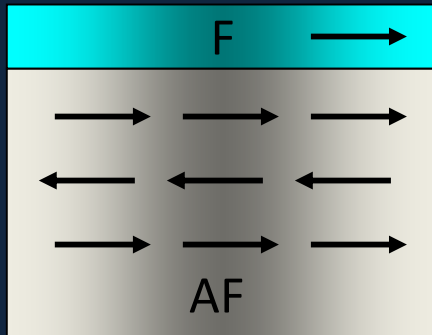
oxidation, dimensionality, charge transfer



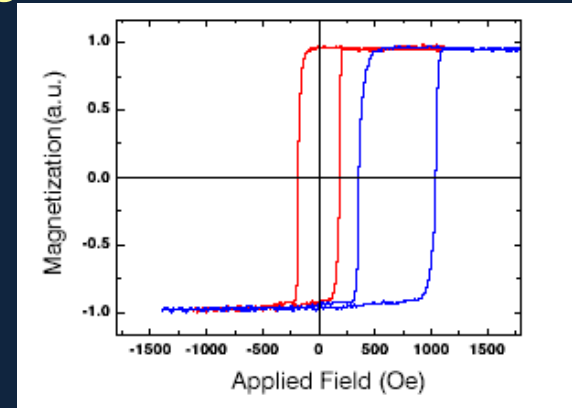
Fe/NiO

motivation

F/AF interface – exchange bias

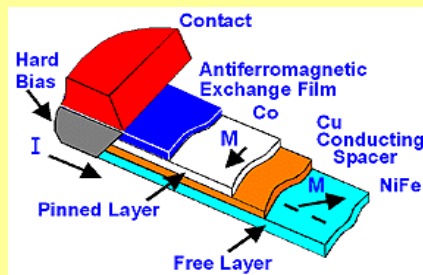


heating up to T_N
+
cooling in H



exchange bias

pinning of the magnetization of one of the FM layers in magnetoresistive devices



extra source of anisotropy to shift the SPM limit in ultrahigh density magnetic memories

V. Skumryev et al., *Nature* 423 (2003) 850.

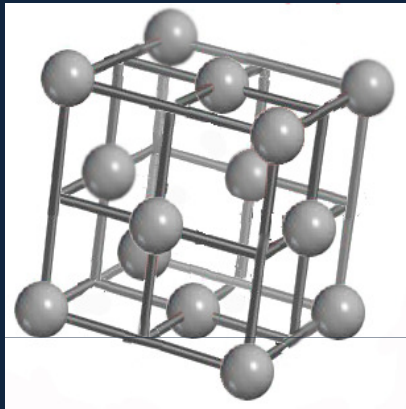
- no complete and quantitative physical model of exchange bias
- strong dependence on the structure of the interfaces



study of atomic-scale characterized systems

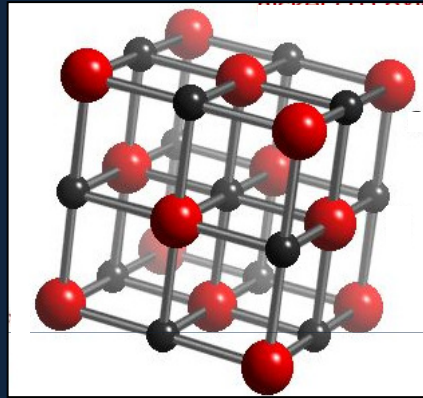
structure

Ag



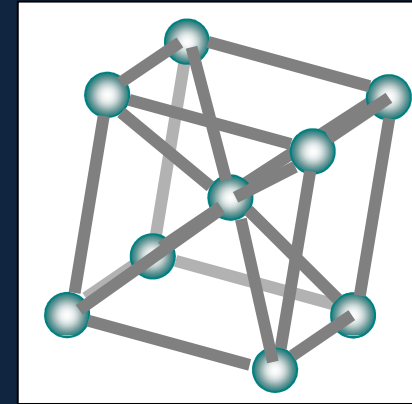
$$a_{\text{Ag}} = 4.086 \text{ \AA}$$

NiO



$$a_{\text{NiO}} = 4.176 \text{ \AA}$$

Fe



$$a_{\text{Fe}} = 2.866 \text{ \AA}$$
$$d_{\text{Fe}} = 4.053 \text{ \AA}$$

$$m_{\text{NiO-Ag}} \sim 2\%$$

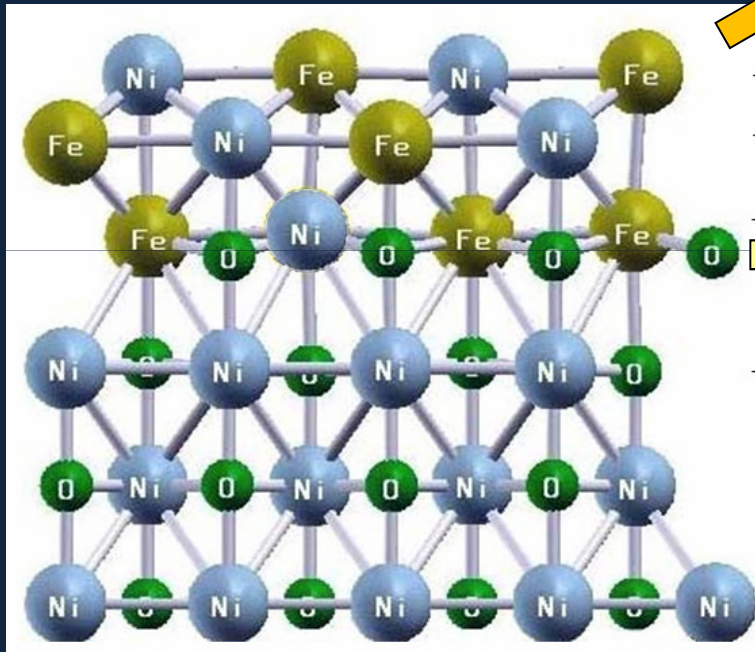
$$m_{\text{Fe-NiO}} \sim 3\%$$

Fe
NiO
Ag(001)

epitaxial system

$$\text{NiO } T_N = 520 \text{ K} \gg \text{RT}$$

previous studies



bcc Fe-Ni alloy formation (3 ML)

P. Luches et al., Surf. Sci. 532 (2003) 409.
S. Benedetti et al., Surf. Sci. 572 (2005) L348.

planar FeO-like phase

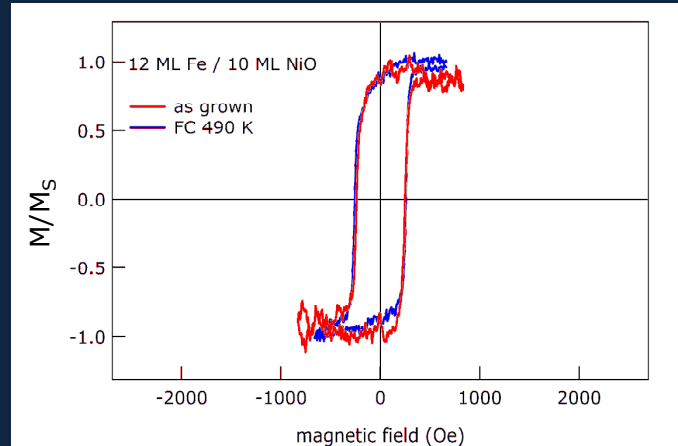
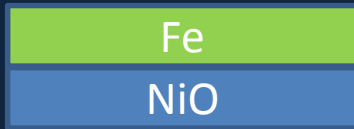
P. Luches et al., Phys. Rev. Lett. 96 (2006) 106106.

NiO reduction+ Fe oxidation

T.J. Regan et al., Phys. Rev. B 64 (2001) 214422.
R. De Masi et al. Surf. Sci. 513 (2002) 523.

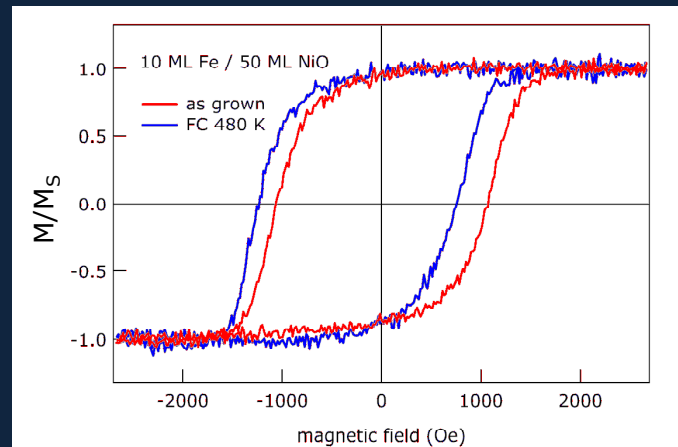
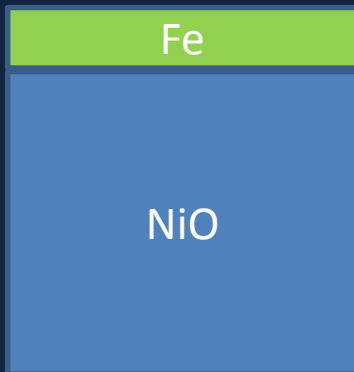
magnetic properties

MOKE



$H_{EB} = 0 \text{ Oe}$

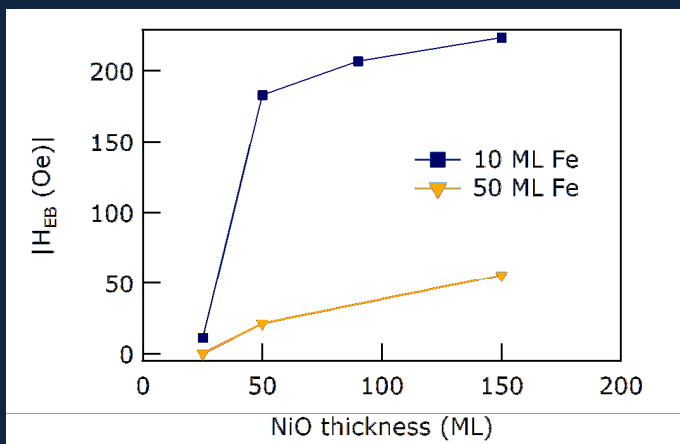
no EB for $t_{\text{NiO}} \leq 25 \text{ ML}$



$H_{EB} = -220 \text{ Oe}$

magnetic properties

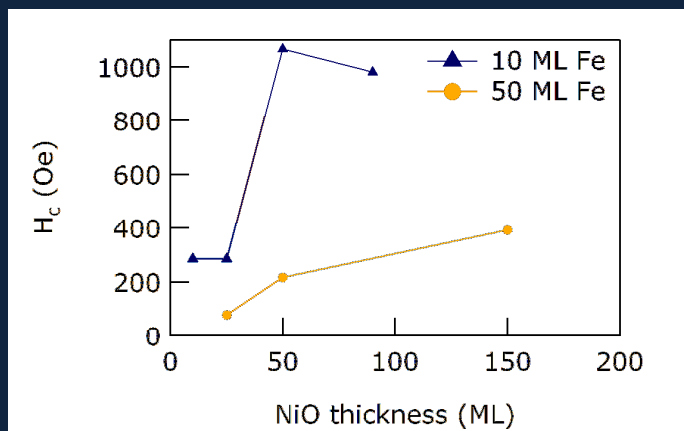
exchange bias



role of the interface

oxidized Fe phase
uncompensated moments in NiO

coercive field



depth resolved magnetic
characterization by NRS

experimental



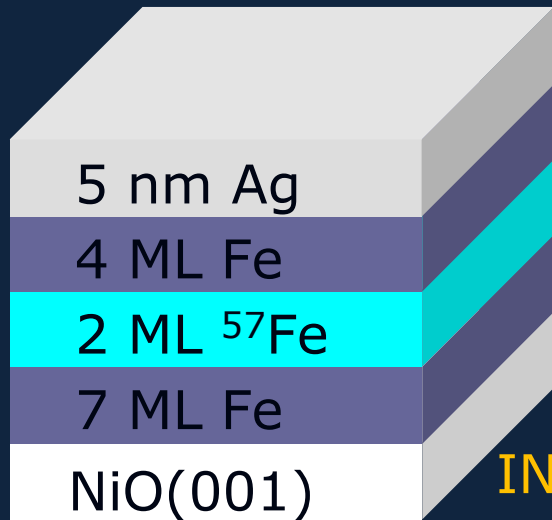
IF-sample

growth conditions

Substrate: Ag(001)

NiO: $R_{\text{Ni}} \sim 1 \text{ \AA}/\text{min}$ $P_{\text{O}_2} \sim 1 \times 10^{-7} \text{ torr}$
 $T_{\text{Ag}} = 460 \text{ K}$

Fe: $R_{\text{Fe}} \sim 1 \text{ \AA}/\text{min}$ RT

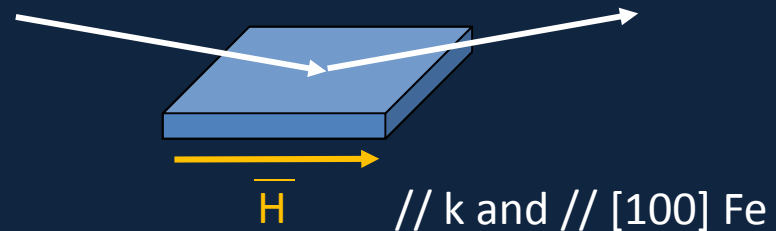


IN-sample

+ NRS measurements

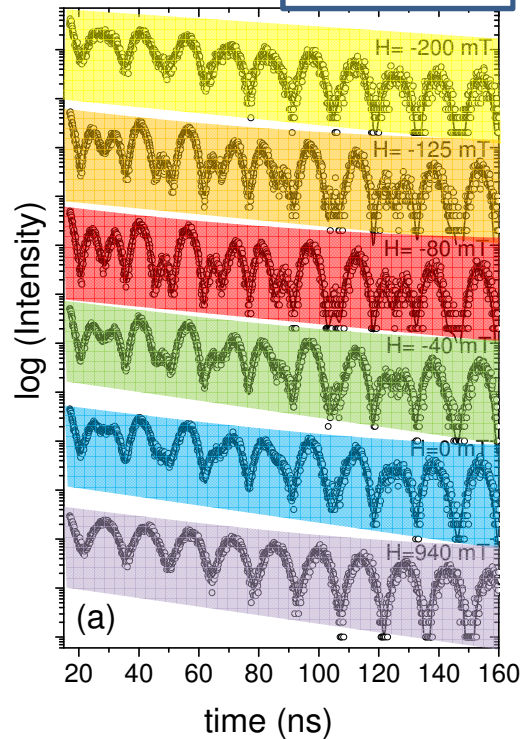
@ ESRF ID18

$h\nu = 14.4 \text{ keV}$ $\Delta t = 176 \text{ ns}$

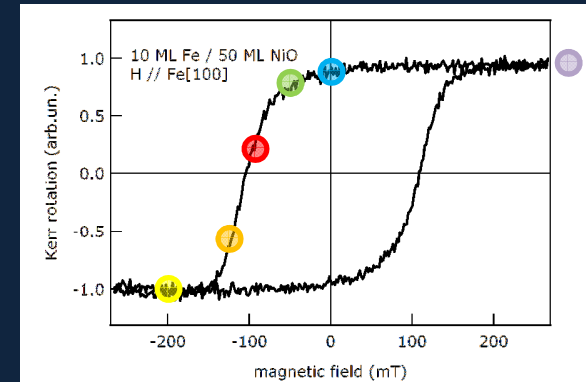
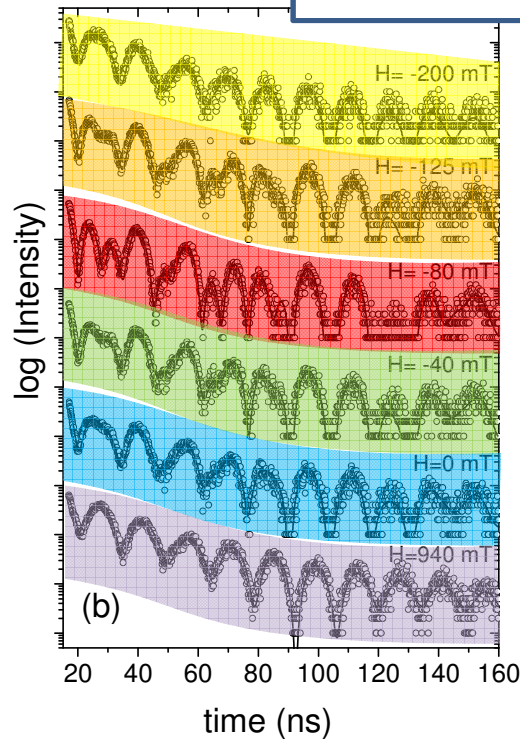
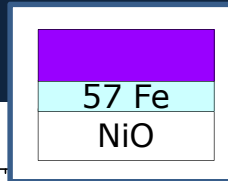


NRS data

IN-sample



IF-sample



fit by NRS package
by C. L'abbe

W. Sturhan, HH 125 (200) 149

Sample	Component #	IS (mm/s)	B_{HF} (T)	$\Delta B_{HF} / B_{HF}$ (%)	RW (%)
IN	1	0 fixed	-33.2 (2)	2	100
IF	1	0 fixed	-33.5 (2)	6 (1)	60 (6)
	2	0.42 (5)	-37.2 (3)	11 (2)	20 (2)
	3	0.42 (5)	+25.3 (5)	90 (5)	20 (2)

metallic

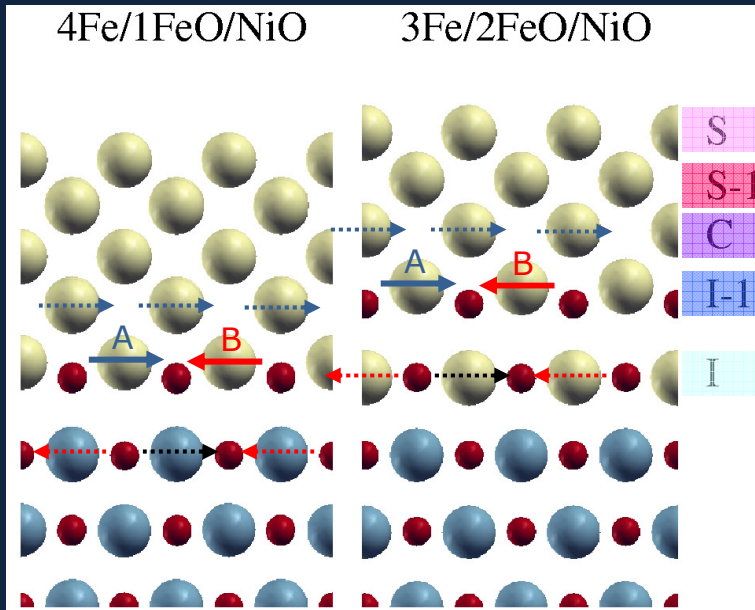
metallic

oxidized

large $|B_{HF}|$

comparison with theory

DFT APW+lo GGA



$$B_{hf} = B_C + \cancel{B_{dip}} + \cancel{B_{orb}}$$

$$B_C = B_{core} + B_{val}$$

$$B_{val} = B_{LOC} + B_{NON-LOC}$$

$$|B_A| = |B_{core} + B_{LOC} + 4B_{NN}|$$

$$|B_B| = |B_{core} + B_{LOC} - 4B_{NN}|$$

asymmetry in positive and negative B_{hf}

System	4Fe/1FeO/NiO		3Fe/2FeO/NiO	
	$B_{HF}(T)$	$m(\mu_B)$	$B_{HF}(T)$	$m(\mu_B)$
S	-24,-25	2.9	-22,-22	3.0
S-1	-37,-37	2.4	-37,-33	2.5
C	-32,-28	2.5	-25,-25	2.7
I-1	-31,-30	2.4	-37,+14	3.1
I	-37,+17	3.1	-35,+37	3.5

NRS

Sample	Component #	IS (mm/s)	$B_{HF}(T)$	$\Delta B_{HF}/B_{HF}(\%)$	RW (%)
IF	1	0 fixed	-33.5 (2)	6 (1)	60 (6)
	2	0.42 (5)	-37.2 (3)	11 (2)	20 (2)
	3	0.42 (5)	+25.3 (5)	90 (5)	20 (2)

S. Blügel et al., PRB 35 (87) 3271

AFM config. for Fe atoms in FeO

⇒ antiferromagnetic FeO phase

summary

CeO₂

- CeO₂(111) films with wide flat terraces can be obtained on Pt(111)
- the Ce³⁺ concentration in the films can be reversibly modified by thermal treatments in UHV or O₂
- Ag nanoparticles reduce ceria and have a higher 3d BE than the bulk

Fe/NiO

- an antiferromagnetic Fe oxide layer is present at the interface
- DFT calculations can be of great help to interpret the NRS data

People

@ S3

Sergio Valeri

Stefania Benedetti

Federico Pagliuca

Sergio D'Addato

Alessandro di Bona

Salvatore Altieri

Federico Boscherini

Luca Pasquini

University of Bologna, Italy

Rudolf Ruffer

ESRF, Grenoble, France

J. Korecki

AGH and ISSC, Krakow, Poland

Theory: Valerio Bellini and Franca Manghi